

Lasers in Manufacturing Conference 2021

The effect of temperature and joining speed on the joining quality for conduction laser joining of metals to polymers

Mahdi Amne Elahi^{a,*}, Max Hennico^a, Peter Plapper^a

^aUniversity of Luxembourg, 6, rue Coudenhove-Kalergi, L-1359 Luxembourg

Abstract

Laser joining of metals to polymers offers several advantages to produce lightweight hybrid assemblies. An important one is the exceptional control over the heat input which defines the temperature at the interface of the materials. Initially, the in-situ heating observation of PA inside ESEM is considered. Then, aluminum and polyamide are joined in an overlap configuration while the temperature was recorded simultaneously at different areas between the materials. The results show that due to excessive heat input, polyamide degrades and leaves bubbles in the melted area. Finally, the materials are laser joined with several joining speeds to investigate different cooling rates of the polyamide during the joining process. It is concluded that joining with high cooling rates generates an amorphous melted layer of the polyamide which is different from the semi-crystalline structure of the bulk. This difference acts as a stress concentration zone and reduces the shear strength of the assembly.

Keywords: metal to polymer laser joining; temperature measurement; polyamide degradation, shear strength.

1. Introduction

To use the laser joining process as a promising technique and provide lightweight assemblies, high mechanical properties of the joints are required. In this regard, surface pre-treatment is crucial. Thanks to the flexibility and versatilities of the laser beam, it can be used for surface treatment besides the joining process to improve the adhesion and mechanical properties of the joints. Nevertheless, it is essential to consider the heat sensitivity of the polymeric material and try to achieve robust joints without degradation of the polymer. When PA6.6 is maintained at 270 °C in a nitrogen atmosphere, no mass reduction or degradation can be observed. However, the mass reduction starts at 300 °C, and at 330 °C rapid degradation occurs. Therefore,

* Corresponding author. Tel.: +352-466644-5885; fax: +352-466644-35885.
E-mail address: mahdi.amneelahi@uni.lu

PA6.6 is a heat-sensitive material. Some studies discussed the temperature measurement during the joining process and the presence of bubbles near the interface of metal/polymer due to polymer thermal pyrolysis.

Schricker et al. studied the effect of polymer heating during the laser joining process on morphology and mechanical properties. Amne Elahi et al. also reported on the formation of an amorphous layer of PA due to the high cooling rate of the laser joining process.

Therefore, it seems interesting to perform an in-situ observation on the polymer behavior with the increase of temperature and try to replicate similar critical temperatures during the laser joining process. In the next step, the effect of the cooling rate should be investigated while thermal degradation of the polymer is suppressed. And finally, the effect of different polymer morphology near the metal/polymer interface on the mechanical properties of the joints should be studied. With these motivations and objectives, the following experiments are conducted.

2. Experimental procedure

2.1. Materials

For the experiments, aluminum (Al) (1 mm thickness) and polyamide 6.6 (PA) (4 mm thickness) are used. The nominal properties of materials are presented in Table 1. To minimize the humidity content, the PA samples were treated based on the ISO-1110 standard. All samples were cleaned with ethanol directly before further processing. To join Al to PA, the surface of Al samples is pre-treated with the laser polishing process under atmospheric environment to create an artificial Al oxide layer and provide a robust join between the materials.

Table 1. Properties of Al and PA were used in the study.

Property	1050-H24 Aluminum	Polyamide 6.6
Density	2.71 g/cm ³	1.15 g/cm ³
Melting point	650 °C	260 °C
Modulus of elasticity	71 GPa	3.3 GPa
Tensile strength	100 MPa	85 MPa

2.2. In-situ heating of PA inside ESEM

The PA material which is used for this study was evaluated by in-situ heating inside Environmental Scanning Electron Microscopy (ESEM) with FEI ESEM Quanta 400 FEG. The observation during heating the material from 25 to 379 °C was recorded.

2.3. Temperature measurements

Fig 1 depicts the schematics of the joining configuration and the fixture for the temperature measurements and joining processes. The laser joining process was done with a continuous wave (CW) fiber laser with the maximum power of 400 W and a wavelength of 1070 nm. The fiber laser has been combined with a scanner head so the beam quality of $M^2=1.03$ and the spot size of 30 μm were achieved. The joining process was implemented under the atmospheric environment. The focal point of the laser beam is on the Al surface and the clamping force applied via pressure blocks during the temperature measurement and joining process is

constant for all samples. The beam trajectory for the temperature measurement process is fixed (zigzag oscillation of the laser beam with 1 mm amplitude, wobble frequency of 50 Hz, and feed rate of 1 mm/s which is described in equation (1).

$$F(x) = \left| \frac{4af}{v_f} \left(x - \frac{v_f}{2f} \right) - 4a \left\lfloor \frac{f}{v_f} \left(x - \frac{v_f}{2f} \right) \right\rfloor - 2a \right| - a \quad (1)$$

a : amplitude [mm]

f : oscillation frequency [Hz]

v_f : feed rate [mm/s]

To measure the temperature accurately during the process, a slow feed rate ($v_f = 1$ mm/s) is required. Three cases of temperature measurement were considered. In the first case (case A), the joining process was tailored to keep the temperature below the melting point of PA for the whole process. For the second one (case B), the temperature should be between the melting and the degradation points of PA while, for the last case (case C), the temperature is always higher than the degradation point of PA.

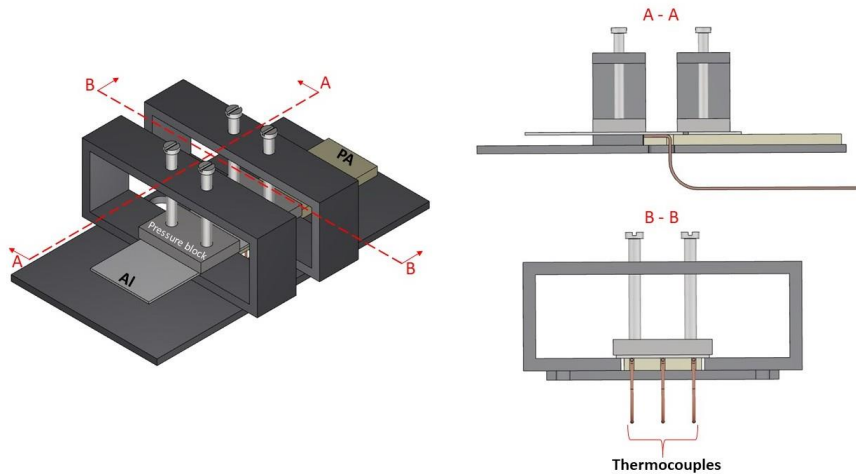


Fig. 1. Schematics of the joining configuration and the fixture for the temperature measurements and joining processes.

Due to the employment of the laser beam in CW with a low feed rate, heat accumulation is inevitable. To moderate the heat accumulation for the temperature measurements, a power ramp for each case is defined as shown in Table 2. For all cases, the temperature is measured at three points (start, middle, and end of the joining area) between Al and PA with K-type thermocouples. The module NI 9219 used for the temperature measurements and recording of the temperature was carried out at a frequency of 50 Hz.

Table 2. Power distribution for all cases of temperature measurement.

	Case A	Case B	Case C
Starting power	130 W	170 W	210 W
Power in the middle of the laser path	140 W	180 W	220 W
Power at the end	0 W	30 W	70 W

The cross-sections of all three cases were studied by Optical Microscopy (OM) with Leica DM 4000 M to evaluate the quality of the joints. A parallel and a perpendicular cross-section (considering the laser path) of each case were prepared from the laser joined samples. Fig 2 shows the schematics of parallel and perpendicular cross-sections.

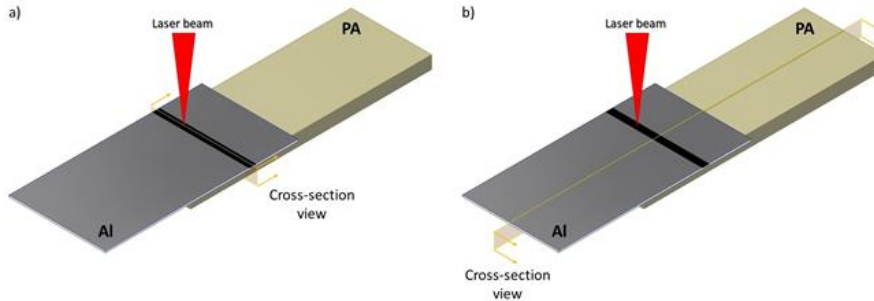


Fig. 2. Schematics of a) a parallel and b) a perpendicular cross-section.

2.4. Different joining speeds and mechanical properties

After observing the PA behavior by increasing the temperature from the room temperature up to 379 °C, it was tried to join Al to PA with different laser feed rates. The feed rates vary between 2 to 120 mm/s and the corresponding laser powers were adapted accordingly to maximize the joining area between Al and PA without PA degradation. For this part of the study, the laser beam was used in CW without any beam trajectory and power ramp. Table 2 depicts the different laser feed rates versus the corresponding power to join Al to PA. The energy input is calculated from equation (2).

$$\text{Energy input [J/mm]} = \frac{\text{Power [W]}}{\text{Feed rate [mm/s]}} \quad (2)$$

Table 2. Different feed rates (joining speed) and the corresponding power following by the energy input for Al to PA joining.

Feed rate [mm/s]	CW laser power [W]	Energy input [J/mm]
2	148	74
5	176	35.2
30	260	8.6
60	328	5.4
90	352	3.9
120	388	3.2

The mechanical properties of the laser joined samples are measured in a single lap shear test assembly and reported in terms of MPa by measuring the maximum shear loads and divide them into the contact areas between Al and PA. The reported values consist of at least five individual measurements for each feed rate.

3. Results and Discussions

3.1. In-situ heating of PA inside ESEM

Fig 3 shows the images of ESEM in-situ heating. They represent the evolution of the PA melting process from room temperature to the melting range followed by the thermal degradation of PA due to excessive heat. The PA starts to melt at approximately 299 °C and at approximately 339 °C the thermal degradation is observed by bubble formation in the molten PA.

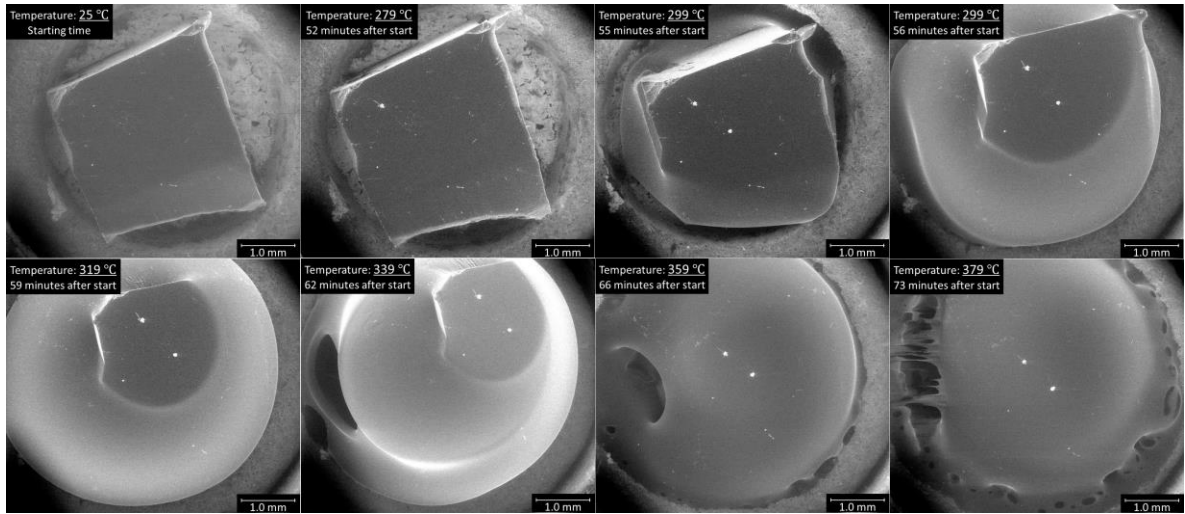


Fig. 3. In situ ESEM heating observation for PA sample.

3.2. Temperature measurements

Fig 4 shows the temperature measurements for Al to PA laser joining for cases A, B, and C. In case A, the measured temperatures for all thermocouples are less than the melting point of PA while, in case B, they are between the melting point and the degradation temperature which are observed in Fig 3, and in case C, all the temperatures are higher than the degradation temperature.

The time of the laser joining process for all cases is 30 seconds (width of Al is 30 mm), and the temperature is measured at the start, middle, and end of contact between Al and PA. The defined power ramp for each case was effective enough to keep a relatively constant temperature from one thermocouple to the next one. It is worth mentioning that without the power ramp, there is considerable damage to the PA at the end of the joining area for all cases and more specifically for case C.

For case A, as the measured temperatures are below the melting point of PA, no robust joint was observed on the cross-sections of the samples.

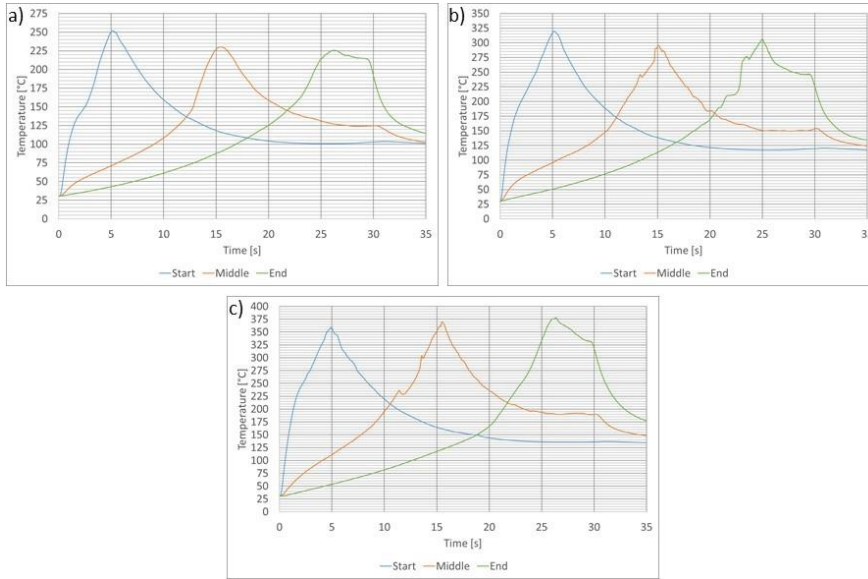


Fig. 4. Temperature measurements for a) case A, b) case B, and c) case C.

Regarding cases B and C, Fig 5 depicts the parallel and perpendicular cross-sections of the corresponding joined samples. For case C, the thermal degradation of PA all along the joining area is visible in the form of bubbles at the melted PA layer near the interface of Al/PA. It is worth mentioning that in some samples small degradation areas of PA were observed for case B. It most probably happened due to the heat accumulation caused by the slow feed rate of the process and the high temperature the thermocouple recorded for the start of the process.

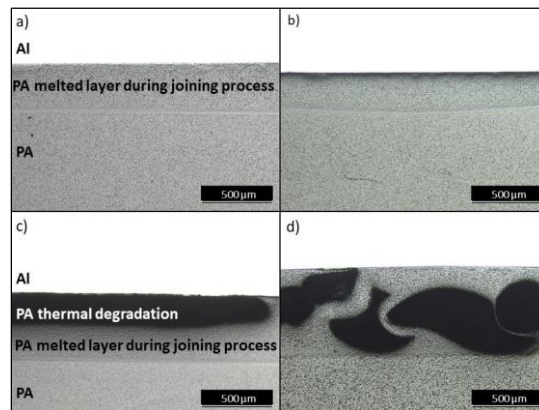


Fig. 5. a) Case B parallel, b) case B perpendicular cross-sections, c) case C parallel, and d) case C perpendicular cross-sections.

Fig 6 shows the depth measurements of PA melted layer from parallel cross-sections of samples laser joined with the parameters of cases B and C. The melted depth of case C is always higher than case B all along the contact area because of higher temperature which leads to a higher volume of melted PA. Due to the high

clamping force applied during the process, the depth of the melted layer is higher at the edges of PA and it follows by ejection of molten PA outside of the contact area which is more extreme in case C.

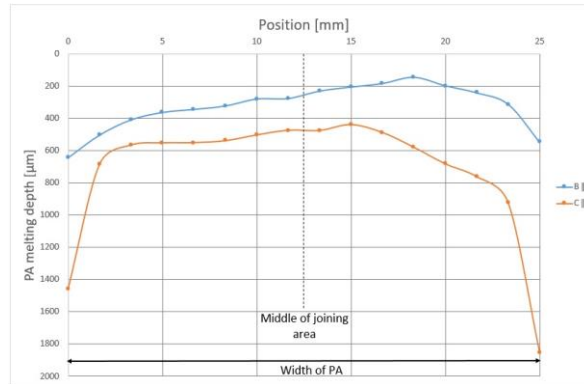


Fig. 6. PA melting depth measurements from parallel cross-sections of cases B and C.

3.3. Different joining speeds and the mechanical properties

As the samples for temperature measurements are produced with a very low feed rate (joining speed), the structure appearance of the re-melted layer is very similar to the bulk PA which is semi-crystalline. It is interesting to investigate the structure of molten PA with different joining speeds. Therefore, Al was joined to PA with different linear feed rates of 2 to 120 mm/s.

Fig 7 presents the cross-section image of the laser-joined samples with the speed of 2, 5, and 30 mm/s. As can be observed, due to the high energy input for joining process of these samples, the depth of the melted layer for 2 and 5 mm/s is visible even with low-magnification images while with higher magnifications due to the similarity of appearances between the melted layer and the bulk PA, the melted layer is less visible. For 30 mm/s joining speed, the melted layer becomes less similar to the bulk PA in appearance.

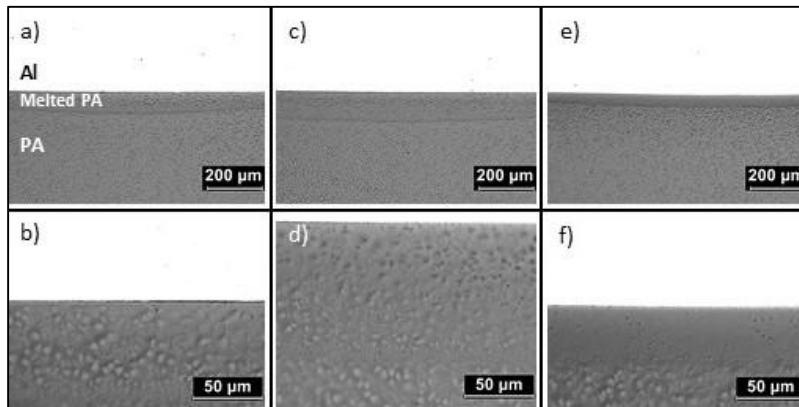


Fig. 7. Perpendicular cross-sections of a) and b) 2 mm/s, c) and d) 5 mm/s, e) and f) 30 mm/s joining speed.

Fig 8 depicts the cross-sections for samples joined with the feed rates of 60, 90, and 120 mm/s. Generally, by increasing the speed from 2 to 120 mm/s the size of the melted layer significantly reduces while the appearance of the layer becomes less similar to the bulk PA. Grazing X-Ray Diffraction (XRD) on the PA material for this study presents 58.5 % crystallinity. The previous investigations by the authors showed that the melted layer corresponding to the laser joining with 112.45 mm/s feed rate is amorphous. It is due to this fact that laser joining with a high feed rate provides a higher cooling rate for the molten PA during the laser joining process. This fact can be discussed from two aspects. First, by joining with high feed rate the total time PA experiences heat via conduction from Al is reduced, and second, the volume of the melted layer is reduced. The combination of the mentioned aspects significantly increases the cooling rate of the molten PA and therefore, generates the amorphous structure for the melted layer.

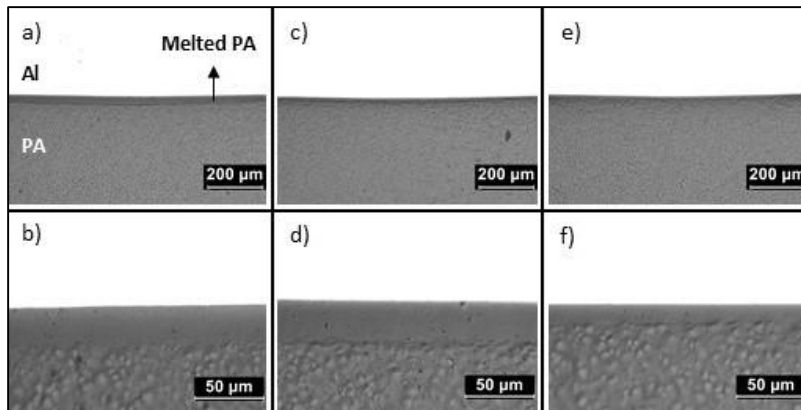


Fig. 8. Perpendicular cross-sections of a) and b) 60 mm/s, c) and d) 90 mm/s, e) and f) 120 mm/s joining speed.

It is reasonable to assume that by reducing the cooling rate of the molten PA due to the lower feed rate and more volume of the molten PA during the joining process, the structure of the melted layer becomes more crystalline. Therefore, the difference between the appearance of the melted layer and the bulk PA becomes less clear. To sum up, for 2 and 5 mm/s joining speed, the appearance of the melted layer is the most similar to the bulk PA while for 90 and 120 mm/s, the layer seems completely different from the bulk in appearance, and it is amorphous. It has been tried to use XRD and quantify the crystallinity percentage of the melted layer with different joining speeds however, it was not successful due to the size of the melted layer and low volume of crystalline phases in that areas. In general, based on the results, the melted layer of the samples with 2 mm/s joining speed is more crystalline than that of 120 mm/s.

Table 3 shows the maximum depth of PA melted layer (middle of the joining area) for different joining speeds which is measured from the cross-sections of the joined samples. As discussed before, generally by reducing the energy input, less volume of PA experiences heat, and therefore the depth of the melted layer should reduce. However, the depth of the PA melted layer for 2 mm/s is lower than that of 5 mm/s. It is due to this fact that Al is a highly reflective material for the near-infrared laser beam and by reducing the laser power significantly, the required power density to form a robust keyhole is missing and consequently, the depth of the keyhole reduces.

Table 3. Depth of PA melted layer for the samples with different feed rates of laser joining.

Feed rate [mm/s]	Depth of PA melted layer [μm]
2	76.8
5	103.7
30	38.9
60	29.7
90	17.8
120	11.4

Fig 10 represents the shear strength of the samples laser joined with different feed rates. It can be observed that by increasing the joining speed the shear strength of the joined samples reduces. A brief comparison between the shear strength of the samples and the appearances of the melted layer of PA in the cross-section images implies that joining with lower speed and consequently providing a more similar structure between the melted layer and the bulk PA, increases the mechanical properties of the joints. However, by increasing the feed rate, the melted layer gradually becomes more amorphous and therefore less similar to the bulk PA. It can act as a stress concentration point and reduces the mechanical properties of the joints.

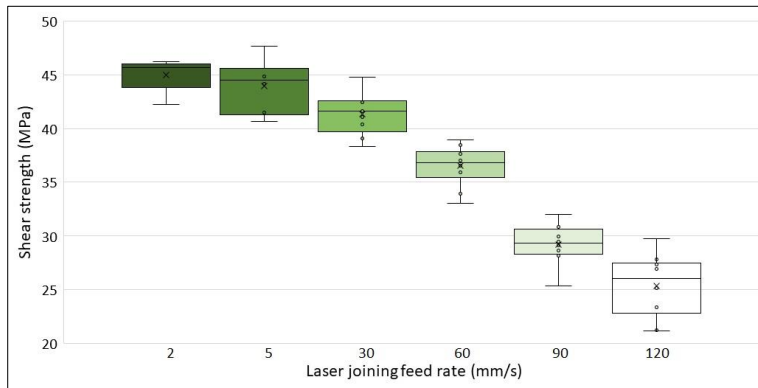


Fig. 10. Shear strength of the samples laser joined with different feed rates.

4. Conclusions

Based on the present study on the temperature measurements and the effect of joining speed for Al-PA laser joining, the followings are concluded:

The PA melts at approximately 300 °C for in-situ heating observation inside ESEM and the temperature measurements with thermocouple during the joining process (the nominal melting point is 260 °C). It follows by thermal degradation at approximately 340 °C. The thermal degradation of PA is observed as bubble formation in the melted areas of PA.

Laser joining of Al to PA with different joining speeds shows that the structure of the PA melted layer is under the influence of the cooling rate. Lower cooling rates provide a more similar structure of melted PA

compared to the bulk PA. For laser joined samples with 2 and 5 mm/s joining speed, the structure of molten PA is the most similar to the bulk PA therefore, the shear strength is at its maximum (approximately 45 MPa). However, for samples joined with 120 mm/s the shear strength is significantly reduced (to approximately 25 MPa) due to the formation of an amorphous layer and stress concentration zone.

Acknowledgments

The presented work is based on “Process Innovation for Sensors in Mobile Applications Based on Laser Assisted Metal-Plastic Joining” project (AFR-PPP grant, Reference 11633333). We like to thank Marcus Koch (INM - Leibniz Institute for New Materials) for ESEM in-situ heating experiments. The authors would like to thank the support of the Luxembourg National Research Fund (FNR) and acknowledge Cebi Luxembourg as the industrial partner of the project.

References

- Amne Elahi, M., Koch, M., Plapper, P., 2019. Laser polishing of Aluminum and Polyamide for dissimilar laser welded assemblies. *Laser in Manufacturing conference (LiM)*.
- Amne Elahi, M., Koch, M., Plapper, P., 2021. Evaluation of the joint based on different surface conditions for aluminum-polyamide laser welding. *Journal of Laser Applications* 33, 012036.
- Lambiase, F., Gena, S., 2017. Laser-assisted direct joining of AISI304 stainless steel with polycarbonate sheets: Thermal analysis, mechanical characterization, and bonds morphology. *Optics & Laser Technology* 88, p. 205-214.
- Schricker, K., Bergmann, J.P., Hopfeld, M., Spieß, L., 2020. Effect of thermoplastic morphology on mechanical properties in laser-assisted joining of polyamide 6 with aluminum. *Welding in the World*.
- Shamey, R., Sinha, K., 2003. A review of degradation of nylon 6.6 as a result of exposure to environmental conditions. *Review of Progress in Coloration and Related Topics* 33, p. 93-107.
- Xianghu, T., Jing, Z., Jiguo, S., Shanglu, Y., Jialie, R., 2015. Characteristics and formation mechanism of porosities in CFRP during laser joining of CFRP and steel. *Composites: Part B* 70, p. 35-43.